International Journal of Multimedia and Ubiquitous Engineering
Vol.11, No.6 (2016), pp.349-360
http://dx.doi.org/10.14257/ijmue.2016.11.6.31

Image Quality Assessment with Saliency Map in Nonsubsampled Contourlet Transform Domain

Pan Wang[1] , Wei Wu[1,*], Xiaomin Yang[1], Kai Liu[2]
and Gwanggil Jeon[3]

[1]*School of Electronics and Information Engineering, Sichuan University, Chengdu, Sichuan, 610064 P.R.China*

[2]*School of Electrical Engineering and Information, Sichuan University, Chengdu, Sichuan, 610064 P.R.China*

[3]*Department of Embedded Systems Engineering, University of Incheon, 12-1 Songdo-dong, Yeonsu-gu, Incheon406-772, Republic of Korea*
mrwpan@sina.com; { wuwei, arielyang, kailiu}@scu.edu.cn; gjeon@inu.ac.kr

Abstract

Many researchers evaluate images by objective image quality assessments instead of subjective ones. Objective image quality assessment sets up mathematical model according to the human visual system, and it evaluates the image quality through the reference image and the distorted image. The Structural Similarity Index (SSIM) is one of the most classical methods in image quality assessment. However, SSIM has several inherent shortcomings. First, SSIM does not take spatial position, spatial frequency, or direction into account. Second, SSIM considers that different regions in an image have equal importance for overall image quality assessment. Third, it is unreasonable to use fixed parameters for various images. To overcome these shortcomings, we propose a new method of image quality assessment based on Nonsubsampled Contourlet Transform (NSCT). Firstly, NSCT is performed to decompose the image into a low-pass map and high-pass ones. Then, low-pass and high-pass maps are respectively assessed with different strategies. In addition, saliency map is added to describe the importance of different regions in an image. Last, we proposed an approach to calculate the adaptive parameters for various images. Experimental comparisons among five public benchmark databases demonstrate that the proposed method is better than other competing methods.

Keywords: *Image quality assessment (IQA), Nonsubsampled Contourlet Transform (NSCT), saliency map*

1. Introduction

Objective image quality assessment aims to adopt the properties of Human Visual System (HVS) to evaluate images, which are distorted during acquisition, processing, compression, storage, *etc.* The objective image quality metrics can be classified into three types, namely, full-reference (FR) metrics, reduce-reference (RR) metrics, and no-reference (NR) metrics.

FR needs to provide a complete reference image. RR means that the reference image is only partially available, while NR means that the reference image is totally not available. Figure 1 shows the three different types of the objective image quality according to the availability of the reference image. In this paper, our work focuses on full-reference metrics.

The traditional objective image quality assessment includes mean squared error (MSE)

*Corresponding Author

ISSN: 1975-0080 IJMUE

and peak signal to noise rate (PSNR). Those early methods are widely used because they are simple to calculate, and they have clear physical meanings. However, those methods do not take the model of HVS into account. It results that they do not match the human subjective evaluation [1-9]. To overcome this problem, many researchers proposed many new methods to simulate HVS, such as noise quality measure (NQM) [10], visual signal-to-noise ratio (VSNR) [11] and information fidelity criterion (IFC) [12]. However, these new methods do not perform well due to the complexity of HVS until the structural similarity index (SSIM) [13] rises. The great success of SSIM and its extensions attribute to the hypothesis that HVS is highly adapted for extracting structural information from the image.

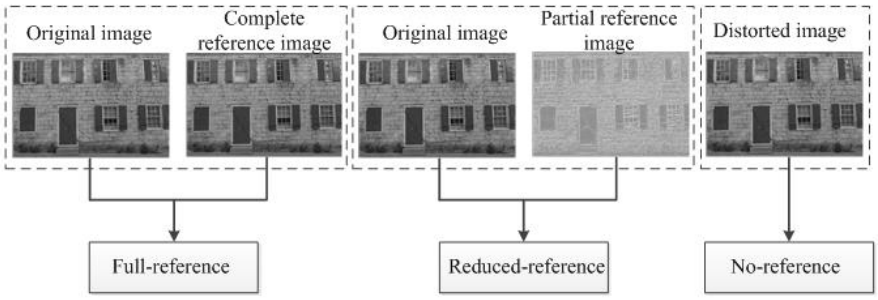

Figure 1. Three Different Types of the Objective Image Quality

We have three main contributions in this paper. First, nonsubsampled contourlet transform was firstly used for image assessment. Nonsubsampled contourlet transform (NSCT), which can effectively capture the multiscale and multidirection information of image, now has been widely used in many image processing applications such as denoising, enhancement and so on. In this paper, we assess the image in NSCT domain rather than spatial domain. Second, we apply a strategy to assign different regions into different weights, because from a perceptual point of view, different regions of an image may have different importance. Thus, it is reasonable to give different weights to different regions when evaluating the image quality. Visual saliency tries to replicate the HVS attention process through saliency map, which emphasizes the more important regions of an image from a perceptual point of view [14]. Third, we propose an approach to adaptively adjust the parameters for different images, since those different images may have different properties. Different from existing methods, which are with same parameters for different images, the proposed method is with adaptive parameters.

In this paper, we propose a new FR image quality assessment (IQA) metric, namely NSCT-SSIM, by combining NSCT and saliency map. The proposed method not only integrates NSCT into the image quality assessment, but also introduces saliency map to measure the different importance of different regions. Furthermore, we propose a strategy, which apply adaptive parameters instead of fixed parameters to different images.

This paper is organized as follows. In Section 2, we describe nonsubsampled contourlet transform and saliency map respectively. In Section 3, we introduce the image quality assessment proposed on the basis of nonsubsampled contourlet transform (NSCT-SSIM). In Section 4, we present the experimental results of the method proposed and related discussions. In Section 5, we draw the conclusion of this paper.

2. Mathematical Theory

First we briefly introduce the nonsubsampled contourlet transform in this section. Subsequently, we describe the saliency maps.

2.1. The Non-subsampled Contourlet Transform

The contourlet transform was proposed by Do *et al* [15]. The contourlet transform, which is a real 2D image representation, consists of a Laplacian pyramid (LP) and a direction filter bank (DFB). The transform has the properties of multiscale, localization, multidirection, and anisotropy. Though the contourlet transform can capture the intrinsic geometric structures such as contours in all directions, it is lack of shift-invariance because of the downsampling and upsampling.

The nonsubsampled contourlet transform (NSCT) [16-17], which is a fully shift-invariant, multiscale, and multidirection expansion, proposed by Cunhato, solves this problem perfectly. The NSCT is constructed by the nonsubsampled pyramid (NSP) and the nonsubsampled directional filter bank (NSDFB) as shown in Figure 2.

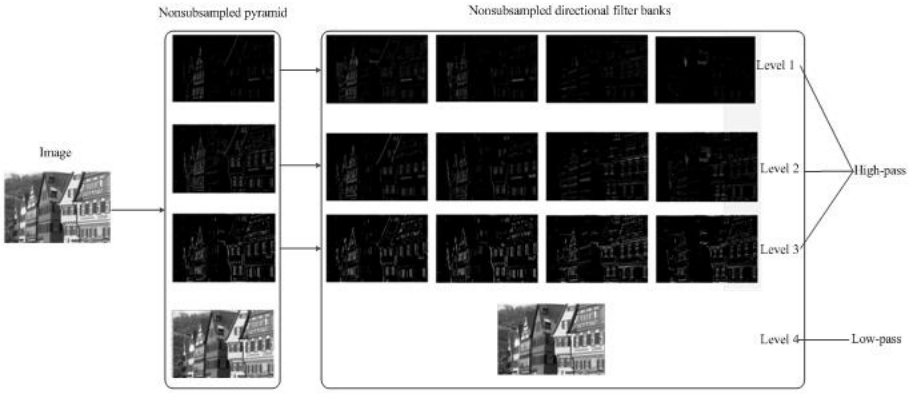

Figure 2. Flow Chart of Nonsubsampled Contourlet Transform

2.2. Saliency Maps

Visual saliency extraction plays an important role in image processing. Many researchers tried to explore the characteristics of the human visual system to computer vision for image analysis. It is given that salient regions can be better perceived by HVS than non-salient regions. In consequence, the observer's judgment of image quality is prejudiced by distortions presented in saliency regions. Following this logic, saliency map extracted from the image can play the fundamental role in improving image quality metrics.

The saliency model used in this paper is proposed by Itti Koch [18]. Itti Koch model is widely adopted due to its simple architecture and its good performance with nature scenes. It is a bottom-up and stimulus-driven approach, which is capable of strong performance even with complex natural scenes. And it combines the multiscale image features adopted by multi-scale analysis to a single topographical saliency map. Itti Koch model is shown in Figure 3.

3. The Proposed Method

In this paper, we propose a new method, namely, NSCT-SSIM, which assesses image quality in NSCT domain rather than spatial domain. The method applies different strategies to low-pass and high-pass maps, which are obtained by performing NSCT. And saliency map is introduced to describe the importance of different regions in an image. Finally, we proposed an approach to adaptively calculate the parameters for various images. The framework of the proposed method is shown in Figure 4. The computation of NSCT-SSIM index consists of five stages. The first stage is to decompose the images into low-pass and high-pass maps through NSCT. The second stage is to calculate the

similarity of low-pass map and high-pass maps. The third stage is to obtain the saliency map of the reference image. The fourth stage is to adaptively select the parameters. The final stage is to integrate the previous four stages into a single similarity score.

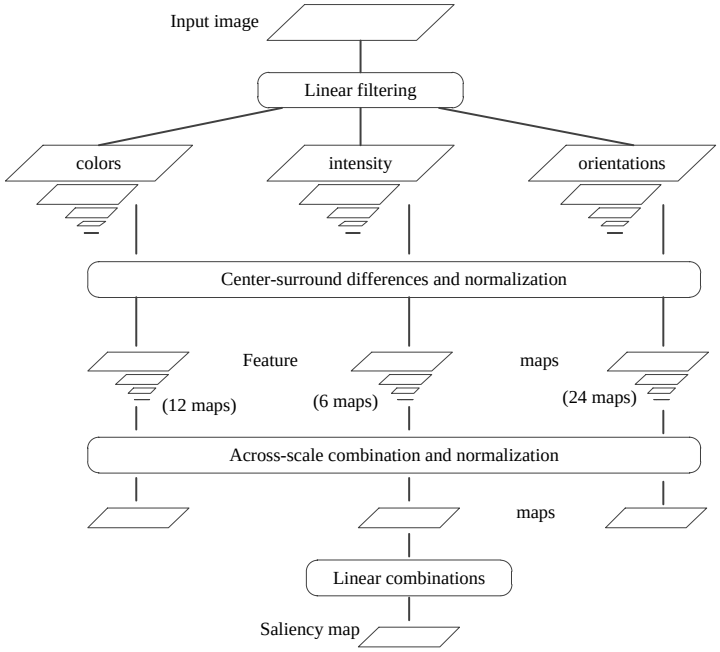

Figure 3. Architecture Comparison of Itti Koch Model

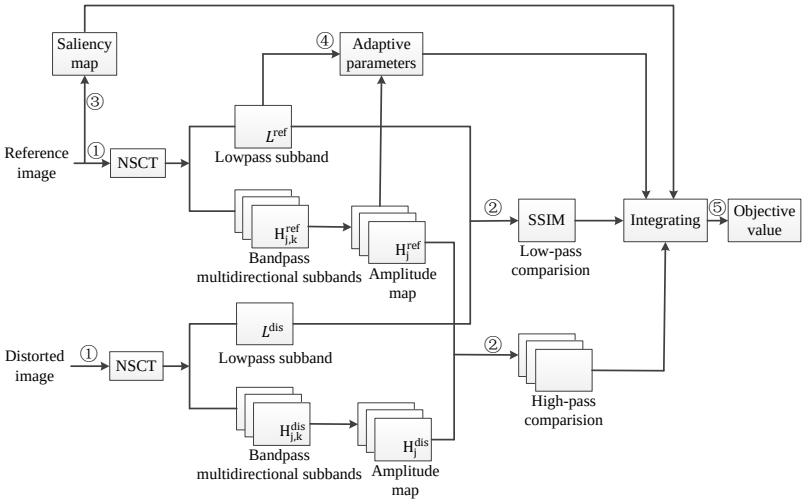

Figure 4. Framework of the NSCT-SSIM Measurement System

Firstly, we perform NSCT to decompose the reference image I^{ref} and the distorted image I^{dis} respectively. Then we can obtain the low-pass and high-pass maps of the reference image and the distorted image.

Secondly, we calculate the similarity maps of low-pass maps and high-pass maps respectively. For low-pass maps, we use the structural similarity measure (SSIM) [19] to calculate the similarity measure between L^{ref} and L^{dis}, *i.e.*, the low-pass maps of the reference image and the distorted image. P^{ref} and P^{dis}, which are derived from the low-pass maps (low frequency NSCT coefficient map) of the reference image I^{ref} and the

distorted image I^{dis} respectively, are two patches. The two patches have been aligned with each other. Suppose that the center of L^{ref} and L^{dis} is at x. The definition of the SSIM metric between L^{ref} and L^{dis} at each point can be expressed as:

$$LPSSIM(L^{ref}(x),\mathrm{L}^{\mathrm{dis}}(x)) = \frac{(2\mu_{L^{ref}}\mu_{L^{dis}} + c_1)(2\sigma_{L^{ref}L^{dis}} + c_2)}{(\mu_{L^{ref}}{}^2 + \mu_{L^{dis}}{}^2 + c_1)(\sigma_{L^{ref}}{}^2 + \sigma_{L^{dis}}{}^2 + c_2)} \quad (1)$$

Where $\mu_{L^{ref}}$ and $\mu_{L^{dis}}$ refer to the respective mean of $L^{ref}(x)$ and $L^{dis}(x)$. $\sigma_{L^{ref}}$ and $\sigma_{L^{dis}}$ denote the respective variance of L^{ref} and L^{dis}. $\sigma_{L^{ref}L^{dis}}$ refers to the covariance of $L^{ref}(x)$ and $L^{dis}(x)$. The small nonnegative constant c_1, c_2 are added for voiding instability when the denominator is nearly close to zero.

For the high-pass maps, we define the similarity measures as follows:

$$HPS_{H_j}(H_j{}^{ref}(x), H_j{}^{dis}(x)) = \frac{AM_j^{ref}(x)AM_j^{dis}(x) + c_3}{(AM_j^{ref}(x))^2 + (AM_j^{dis}(x))^2 + c_3} \quad (2)$$

Where $AM_j^{ref}(x)$, $AM_j^{dis}(x)$ refer to the respective amplitude of the reference image and the distorted image at position *x* on scale *j*. And c_3 is a small positive constant to void instability when the denominator is nearly close to zero. $AM_j^{ref}(x)$, $AM_j^{dis}(x)$ can be calculated as follows:

$$AM_j^{ref}(x) = \sqrt{\sum_{k=1}^{N} H_{j,k}^{ref}(x)^2} \quad (3)$$

$$AM_j^{dis}(x) = \sqrt{\sum_{k=1}^{N} H_{j,k}^{dis}(x)^2} \quad (4)$$

Where $H_{j,k}^{ref}(x)$ refers to the high frequency NSCT coefficients of the reference image of position *x* at direction *k* on scale *j*. Similarly, $H_{j,k}^{dis}(x)$ refers to the high frequency NSCT coefficients of the distorted image of position *x* at direction *k* on scale *j*.

After computing the similarity measures of low-pass maps and high-pass maps at each location, the overall similarity between the reference image and the distorted image can be calculated. The similarity is defined as follows:

$$LHPSSIM(I^{ref}, I^{dis}) = LPSSIM^{\alpha} \cdot [\prod \sum_{j=1}^{N} (HPS_{H_j})^{\gamma_i}] \quad (5)$$

Where α is determined by the importance of low-pass maps, while λ_j is determined by the importance of high-pass maps at level *j*. If low-pass maps are more important, a larger α is needed, and vice versa. Similarly, the more important the high-pass maps are, the larger λ_j is.

Usually, existing methods set the parameters as fixed values. Different from those methods, we adaptively adjust the parameters according to the properties of the image assessed. If an image contains more edge (or detail) information, the image is of more importance. Also if an image contains more edge information, the variance of low-pass map would be larger. Therefore, we propose that the importance of low-pass map is in proportion to the variance $\sigma_{L^{ref}}$. Similarly, we proposed that the importance of high-pass maps is in proportion to the energy. Specifically, λ_j is in proportion to the energy of amplitude map at level *j*.

Thus, α can be calculated as:

$$\alpha = \frac{\sigma_{L^{ref}}}{\sigma_{L^{ref}} + \frac{1}{N}(\sum_{j=1}^{N} E_{H_j})} \tag{6}$$

And λ_j can be expressed as:

$$\lambda_j = (1-\alpha)(\frac{E_{H_j}}{\sum_{j=1}^{N} E_{H_j}}) \tag{7}$$

Herein, E_{H_j} refers to the energy of amplitude map, and it can be calculated as:

$$E_{H_j} = \sum_{x \in \Omega} \left\| H_j^{ref}(I^{ref}) \right\|_2^2 \tag{8}$$

Where N denotes to the layer number of NSCT.

Different regions have different contributions to HVS' perception of an image. The visual saliency map describes the most focused areas in the image, it implies that these areas have a higher impact on HVS when evaluating the similarity between the reference image and the distorted image. Therefore, we use saliency map to weight the importance of saliency regions in the overall similarity between the reference image and the distorted image. In this paper, we calculate saliency map by Itti Koch model [18]. The saliency map of reference image is computed as:

$$S_M = Itti(I^{ref}) \tag{9}$$

where S_M refers to the saliency map of the reference image I^{ref}. Itti refers to the processing procedure of Itti Koch model to obtain the saliency map.

Then the final NSCT-SSIM index between the reference image and the distorted image can be defined as follows:

$$NSCTSSIM = \frac{\sum_{I \in \Omega} LHPSSIM(I^{ref}, I^{dis}) \cdot S_M}{\sum_{I \in \Omega} LHPSSIM(I^{ref}, I^{dis})} \tag{10}$$

4. Experimental Results and Discussion

4.1. Experimental Setup

To validate the performance of the proposed method, we test the method among five famous image databases, which are A57 [20], MICT [21], IVC [22], LIVE [23], and TID2008 [24]. The newly-proposed NSCT-SSIM will be compared with SSIM, IFC, NQM, paired comparison (PC), and PSNR.

In the IQA community, there are four widely-used metrics to evaluate the performance of IQA metrics including Spearman rank-order correlation coefficient (SROCC), Kendall rank-order correlation coefficient (KROCC), Pearson linear correlation coefficient (PLCC), and root MSE (RMSE). PLCC and RMSE both need a nonlinear procedure before calculation. In this paper, we use the following mapping function:

$$f(x) = \beta_1(\frac{1}{2} - \frac{1}{1+e^{\beta_2(x-\beta_3)}}) + \beta_4 x + \beta_5 \tag{11}$$

Where β_i (i = 1-5) are the parameters to be fitted. A better objective IQA measure is expected to have higher SROCC, KROCC, and PLCC values but lower RMSE values.

There are several parameters that need to be determined for the NSCT-SSIM index. In our experiment, the low-pass map of the second layer obtained by nonsubsampled pyramid (NSP) is considered as the map, which is used to measure the similarity of low-pass map. And all the high-pass maps obtained by

nonsubsampled directional filter bank are considered as high-pass maps, which is used to measure the similarity of high-pass maps. We set c_1= 0.01, c_2 = 0.006, c_3 = 80, the layer number N = 3, and the numbers of directions at three scales 2, 4, 8 respectively. These parameters are then fixed for all the following experiments conducted.

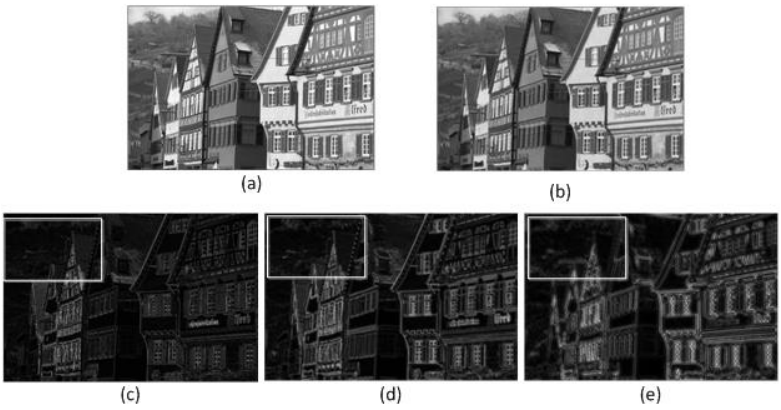

Figure 5. (a) The Reference Image (Kp08) in MICT Database; (b) the Low-Pass Map of (a). (c) to (e) are Corresponding AM Maps in Different Scale of NSCT

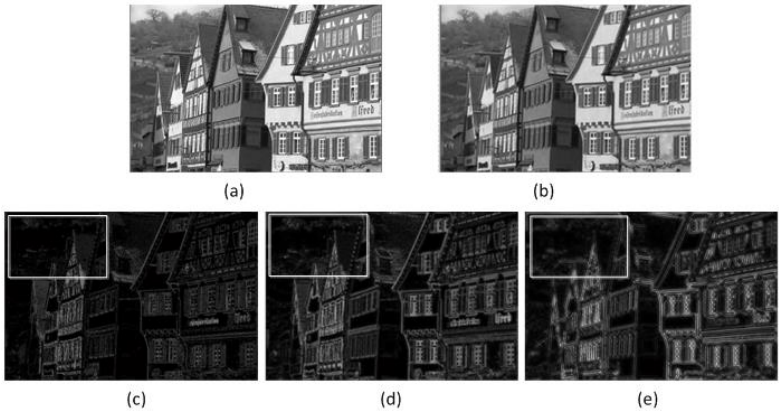

Figure 6. (a) The Distorted Image (kp08_24_jp2) in MICT Database; (b) the Low-Pass Map of (a). (c) to (e) are Corresponding AM Maps in Different Scale of NSCT

Table 1. Performance Comparisons between NSCT-SSIM and Other Methods among Five Databases

		NSCT -SSIM	SSIM	IFC	NQM	PC	PSNR
TID2008	SROCC	0.8222	0.7749	0.5692	0.6243	0.8002	0.5245
	KROCC	0.6270	0.5768	0.4261	0.4608	0.6045	0.3696
	PLCC	0.8294	0.7732	0.7359	0.6135	0.8215	0.5309

	RMSE	0.7596	0.8511	0.9086	1.0598	0.7652	1.1372
LIVE	SROCC	0.9443	0.9479	0.9234	0.9086	0.9150	0.8755
	KROCC	0.7900	0.7963	0.7540	0.7413	0.7581	0.6864
	PLCC	0.9400	0.9449	0.9248	0.8122	0.9265	0.8721
	RMSE	9.3195	8.9455	0.3920	11.193	11.155	13.368
IVC	SROCC	0.9023	0.9018	0.8978	0.8347	0.8981	0.6885
	KROCC	0.7229	0.7223	0.7192	0.6342	0.7121	0.5220
	PLCC	0.9120	0.9119	0.9080	0.8498	0.9076	0.7199
	RMSE	0.4987	0.4999	0.5105	0.6421	0.5115	0.8654
MICT	SROCC	0.9140	0.8794	0.8387	0.8911	0.8709	0.6163
	KROCC	0.7427	0.6939	0.6413	0.7219	0.6819	0.4447
	PLCC	0.9207	0.8887	0.8434	0.8955	0.8750	0.6426
	RMSE	0.4883	0.5738	0.6723	0.5569	0.6058	0.9588
A57	SROCC	0.8076	0.8066	0.3185	0.7981	0.8433	0.6130
	KROCC	0.6142	0.6058	0.2378	0.5932	0.6576	0.4309
	PLCC	0.8020	0.8017	0.4548	0.8020	0.8534	0.6587
	RMSE	0.1468	0.1469	0.2189	0.1468	0.1281	0.1849

4.2. Examples of Effectiveness Validation

In this subsection, examples are used to demonstrate the effectiveness of the proposed method in evaluating the perceptible image quality. Figure 5(a) is the kp08 reference image in the MICT database, and Figure 5(b) is the corresponding low-pass map of the reference image. Figure 5(c) to (e) show amplitude maps of multidirection high-pass maps from scale 1 to scale 3. Figure 6(a) is the kp08_24_jp2 distorted image in the MICT database. The distortion type of Figure 8(a) is "JPEG2000 compression". Figure 6(b) is the corresponding low-pass map of the distorted image. Figure 6(c) to (e) show amplitude maps from scale 1 to scale 3 respectively. The newly-proposed NSCT-SSIM attributes its success to decomposing the image into low-pass map and high-pass ones. By visual examination, in Figure 6(c) to (e), the housetop regions marked by white rectangles have a perceptible difference from the same regions in Figure 5(c) to (e). Accordingly, we can draw the conclusion that high-pass maps in different scales can convey different high frequency details of the same image.

4.3. Evaluation Performance Comparison

This part, we compare the general performance of the competing IQA metrics. Table 1 lists the SROCC, KROCC, PLCC, and RMSE results of NSCT-SSIM and other IQA algorithms on the MICT, IVC, LIVE, A57, and TID2008 databases. The best results are highlighted in boldface for each database. From the experimental results summarized in Table 1, we can find out that the proposed method achieves the best results on almost all the databases except LIVE database, though it achieves a little worse results than the SSIM does on LIVE database. On the whole, we can draw the conclusion that the proposed method achieves the most consistent and stable performance across all the five databases.

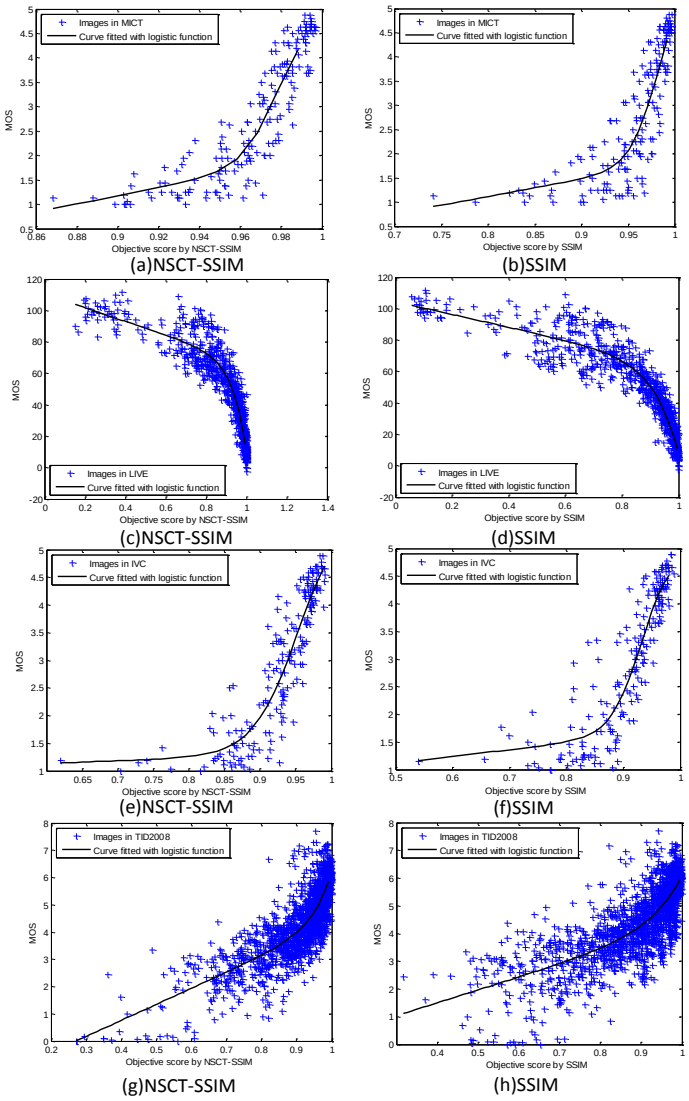

Figure 7. Scatter Plots of Subjective MOS versus Model Prediction Obtained by on Different Databases. (a) NSCT-SSIM on MICT, (c) NSCT-SSIM on LIVE, (e) NSCT-SSIM on IVC, (g) NSCT-SSIM on TID2008, (b) SSIM on MICT, (d) SSIM on LIVE, (f) SSIM on IVC, (h) SSIM on TID2008

In order to verify the method more intuitively, the scattering distributions of subjective MOS versus the predicted scores by NSCT-SSIM and other indices on the MICT, LIVE, IVC, and TID2008 databases are shown in Figure 7. In Figure 7, each red "+" denotes one distorted image, the blue curve is a fitting curve obtained by a nonlinear fitting according to Equation (13). Horizontal and vertical axes respectively denote the given objective quality score and corresponding MOS. From Figure 9, we can see that the fitting results predicted in (a), (c), (e), and (g) are better than those in (b), (d), (f), and (h) respectively. Hence, the experiments above show our algorithm is better than SSIM and other algorithms mentioned.

From the discussion above we can draw a conclusion that the proposed method is more consistent with the subjective scores than other indices be.

5. Conclusion

In this paper, we propose a fresh image quality assessment, namely, NSCT-SSIM index. It is based on the idea that HVS perceives an image mainly depending on its low-pass map and high-pass maps as well. The low-pass maps convey the information of luminance, contrast, and structural similarity. While the high-pass maps contain different direction and can complementarily interpret the high frequency information. In addition, we introduce the saliency map to determine the importance of the different regions. One of the factors of success for NSCT-SSIM is that we adaptively calibrate the weighting parameters for different applications. Experiments show that the proposed method can consistently perform well across almost all the testing databases, and it is validated that it is a very robust IQA metric.

Acknowledgments

The research is sponsored by the National Natural Science Foundation of China (No. 61271330 and No. 61411140248), the Science and Technology Plan of Sichuan Province (No. 2014GZ0005), the Scientific Research Foundation for the Returned Overseas Chinese Scholars, State Education Ministry, the National Science Foundation for Postdoctoral Scientists of China (No. 2014M552357), and the Research Fund for the Doctoral Program of Higher Education (No. 20130181120005).

References

[1] B. Girod, "What's wrong with mean-squared error", in Digital Images and Human Vision, A. B. Watson, Ed. Cambridge, MA: MIT Press, **(1993)**, pp. 207–220.
[2] P. C. Teo and D. J. Heeger, "Perceptual image distortion", in Proceeding SPIE, vol. 2179, **(1994)**, pp. 127-141.
[3] A. M. Eskicioglu and P. S. Fisher, "Image quality measures and their performance", IEEE Trans. Commun., vol. 43, **(1995)**, pp. 2959-2965.
[4] M. P. Eckert and A. P. Bradley, "Perceptual quality metrics applied to still image compression", Signal Processing, vol. 70, **(1998)**, pp. 177–200.
[5] S. Winkler, "A perceptual distortion metric for digital color video", in Proceeding SPIE, vol. 3644, **(1999)**, pp. 175–184.
[6] Z. Wang, "Rate scalable Foveated image and video communications", Ph.D. dissertation, Dept. Elect. Computer Eng., Univ. Texas at Austin, Austin, TX, **(2001)**.
[7] Z. Wang and A. C. Bovik, "A universal image quality index", IEEE Signal Processing Letters, vol. 9, pp. 81–84, **(2002)**.
[8] Z. Wang, "Demo Images and Free Software for "a Universal Image Quality Index", [Online] Available:http://anchovy.ece.utexas.edu/~zwang/research/quality_index/demo.html.
[9] Z. Wang, A. C. Bovik and L. Lu, "Why is image quality assessment so difficult", in Proceeding IEEE Int. Conf. Acoustics, Speech, and Signal Processing, Orlando, FL, vol. 4, **(2002)**, pp. 3313–3316.
[10] N. D. Venkata, T. D. Kite, W. S. Geister, B. L. Evans and A. C. Bovik, "Image quality assessment based on a degradation model", IEEE Trans Image Process, vol. 9, no. 4, **(2000)**, pp. 636-50.
[11] D. M. Chandler and S. S. Hemami, "VSNR: a wavelet-based visual signal-to-noise ratio for natural image", IEEE Trans Image Process, vol. 16, no. 9, **(2007)**, pp. 2284-98.
[12] H. R. Sheikh, A. C. Bovik and G. de Veciana, "An information fidelity criterion for image quality assessment using natural scene statistics", IEEE Trans Image Process, vol. 14, no. 12, **(2005)**, pp. 2117-28.
[13] Z. Wang, A. C. Bovik, H. R. Sheikh and E. P. Simoncelli, "Image quality assessment: From error visibility to structural similarity", IEEE Trans. Image Process., vol. 13, no. 4, **(2004)**, pp. 600-612.
[14] S. Frintrop, E. Rome and H. I. Christensen, "Computational visual attention systems and their cognitive foundations: A survey", ACM Transactions on Applied Perception (TAP), **(2010)**.
[15] M. N. Do and M. Vetterli, "The contourlet transform: An efficient directional multiresolution image representation", IEEE Trans Image Process, vol. 14, no. 12, **(2005)**, pp. 2091-2106.
[16] A. L Cunha, J. Zhou and M. N. Do, "The nonsubsampled contourlet transform: theory, design and applications", IEEE Trans Image Process, vol. 15, no. 10, **(2006)**, pp. 3089-3101.
[17] G. Jeon, "Contrast Intensification in NTSC YIQ", International Journal of Control and Automation, vol. 6, no. 4, **(2013)**, pp. 157-166.
[18] L. Itti, C. Koch and E. Niebur, "A model of saliency-based visual attention for rapid scene analysis", Pattern Analysis and Machine Intelligence, IEEE Transaction on, **(1998)**.

[19] Z. Wang, L. Lu, A. C. Bovik and E. P. Simoncelli, "Image quality assessment: From error measurement to structural similarity", IEEE Trans. Image Processing, vol. 13, **(2004)**.
[20] D. M. Chandler and S. S. Hemami, "A57 Database 2007 [Online]", Available: http://foulard.ece.cornell.edu/dmc27/vsnr/vsnr.html, **(1998)**.
[21] Y. Horita, K. Shibata, Y. Kawayoke and Z. M. P. Sazzad, "MICT Image Quality Evaluation Database 2000 [Online]", Available: http://mict.eng.u-toyama.ac.jp/mict/index2.html.
[22] A. Ninassi, P. Le Callet and F. Autrusseau, "Subjective Quality Assessment-IVC Database 2005 [Online]", Available: http://www2.irccyn.ecnantes.fr/ivcdb.
[23] H. R. Sheikh, K. Seshadrinathan, A. K. Moorthy, Z. Wang, A. C. Bovik and L. K. Cormack, "Image and Video Quality Assessment Research at LIVE 2004 [Online]", Available: http://live.ece.utexas.edu/research/quality.
[24] N. Ponomarenko, V. Lukin, A. Zelensky, K. Egiazarian, M. Carli and F. Battisti, "TID2008—A database for evaluation of full-reference visual quality assessment metrics", Adv. Modern Radioelectron., vol. 10, pp. 30–45, 2009.

Authors

Pan Wang received his BS degree of Information Engineering from Xihua University, China in 2012. Now he is a postgraduate in School of Electronics and Information Engineering, Sichuan University. His research interests are image process, computer vision and pattern recognition.

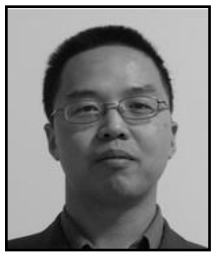

Wei Wu, is currently an Associate Professor in College of Electronics and Information Engineering, Sichuan University, China. He received his BS degree from Tianjin University, China in 1998 and received his MS degree and PhD degrees in communication and information system from Sichuan University China in 2003 and 2008, respectively. He worked in a National Research Council Canada as a post-doctorate in 2009 - 2010. He has published over 50 scholarly papers in academic journals and conferences. He serves as an associate editor of Journal of Pattern Recognition Research. His research interests are image process, computer vision and pattern recognition.

Xiaomin Yang, is currently an Associate Professor in College of Electronics and Information Engineering, Sichuan University. She received her BS degree from Sichuan University, and received PhD degrees in communication and information system from Sichuan University. She worked in University of Adelaide as a post doctorate forone year. She has published over 30 scholarly papers in academic journals and conferences. Her research interests are image process and pattern recognition.

Kai Liu, is currently a professor in the School of Electrical Engineering & Information at the Sichuan University, China. He received the B.S. and M.S. degrees in Computer Science from the Sichuan University, China in 1996 and 2001, and the Ph.D. degree in Electrical Engineering from the University of Kentucky, USA in 2010, respectively. He had been a postdoctoral researcher in the

Information Access Lab at the University of Delaware, USA from Sept., 2010 to Jul., 2011. His main research interests include computer/machine vision, active/passive stereo vision and image processing. His works have been featured in Optics Express, JOSA A, Optics Lett, TPAMI, TIP and SPIE. He is a senior member of IEEE.

Gwanggil Jeon, received the BS, MS, and PhD (summa cum laude) degrees in Department of Electronics and Computer Engineering from Hanyang University, Seoul, Korea, in 2003, 2005, and 2008, respectively. From 2008 to 2009, he was with the Department of Electronics and Computer Engineering, Hanyang University, from 2009 to 2011, he was University of Ottawa, as a postdoctoral fellow, and from 2011 to 2012, he was with the Graduate School of Science & Technology, Niigata University, as an assistant professor. He is currently an assistant professor with the Department of Embedded Systems Engineering, University of Incheon, Incheon, Korea. His research interests fall under the umbrella of image processing, particularly image compression, motion estimation, demosaicking, and image enhancement as well as computational intelligence such as fuzzy and rough sets theories. He was the recipient of the IEEE Chester Sall Award in 2007 and the 2008 ETRI Journal Paper Award.

